Emergence and circulation coupling of moist layers over the tropical Atlantic

Marc Prange[1,2], Bjorn Stevens [3], Stefan A. Buehler[1]

[1]Universität Hamburg, Meteorologisches Institut, Bundesstraße 55, 20146 Hamburg, Germany
[2]Program in Atmospheric and Oceanic Sciences, Princeton University, Princeton, NJ, USA
[3]Max Planck Institut für Meteorologie, Bundesstraße 53, 20146 Hamburg, Germany

Key Points:

- Mid-tropospheric moist layers are ubiquitous around the tropical rain belts and their occurrence is subject to a strong seasonal cycle over the Atlantic.
- Moist layers are associated with a more bottom-heavy large-scale circulation, resembling RCE-based results.
- Moist layers south of the Atlantic summer ITCZ are detrained from the ITCZ while moist layers in the north are sourced from the west African monsoon system.

Corresponding author: Marc Prange, mp1506@princeton.edu

Abstract

Mid-tropospheric elevated moist layers (EMLs) near the melting level have been found in various regional observational studies in the tropics. Recently, a preponderance of EMLs in the presence of aggregated convection was found in cloud resolving simulations of radiative convective equilibrium (RCE), highlighting a significant circulation coupling. Here, we present global monthly EML occurrence rates based on reanalysis, yielding a broader view on where and when EMLs occur in the real world. Over the Atlantic, EML occurrence follows an annual cycle that maximizes in summer, aligning with maximized ITCZ intensity and organisation. Resembling the results in RCE, the large-scale circulation over the Atlantic shifts from a deep overturning in January to a bottom-heavy circulation in July. While EMLs embedded in the July cross-equatorial Hadley cell are found to be sourced from the ITCZ, EMLs north of the ITCZ emerge from the strongly sheared zonal flow over West Africa.

Plain Language Summary

In the vicinity of thunderstorms, the atmosphere is typically dry enabling the moist boundary layer top to radiatively cool efficiently. This yields subsidence and surface divergence that is thought to feed moist air near the surface into the thunderstorm, favoring convective aggregation. Recent idealized simulations have shown that more aggregated convection is associated with an enhanced outflow of moist air in the mid-troposphere that inhibits boundary layer cooling and drives an overturning circulation above the boundary layer. Here, we provide a first observational quantification of mid-tropospheric moist layer occurrence globally on an annual time-scale. We find a significant annual cycle over the Atlantic with a maximum in summer, aligning with peak convective activity and organisation of the Atlantic rainbelt. We show that the Atlantic overturning circulation becomes vertically constrained by the moist layers, similar to the idealized simulations. Moist layers embedded in the Atlantic Hadley circulation are likely sourced from convection within the Atlantic rainbelt, while moist layers over the northern sub-tropical Atlantic emerge from zonal wind shear within the West African monsoon system.

1 Introduction

The work of Pierrehumbert (1995) popularized the view of conceptually splitting up the tropical atmosphere into two columns entailing a moist convective region and a dry subsiding region (Miller, 1997; Larson et al., 1999; Kelly & Randall, 2001; Bellon et al., 2003). This view is useful for assessing the tropics in a framework of global radiative-convective equilibrium (RCE), with the dry regions acting as "radiator fins" to send excess energy to space that was obtained in the "furnace" regions of deep convection. Maintaining the picture of the tropics as a two-column model, Kelly and Randall (2001) stress how the intensity of the tropical circulation is crucially dependent on the vertical distribution of free tropospheric water vapor in the subsidence regions. Increased lower free tropospheric humidity enhances radiative cooling and therefore subsidence and local mass flux (see also Fig. 4 of Sokol & Hartmann, 2022), yielding enhanced circulation strength under constant subsidence area. This emphasizes the need for a profound understanding of the subtropical free tropospheric humidity structure to understand the general circulation.

A similar picture of a two-column tropical atmosphere is painted by studies of cloud-resolving simulations run in RCE configuration. Earlier studies that contrasted the equilibrium states between smaller and larger domains at spatial thresholds around 200 km found that convection aggregates on larger domains, yielding a drier free troposphere and a stronger large-scale circulation than non-aggregated convection that is present on smaller domains (Bretherton et al., 2005; C. J. Muller & Held, 2012). This is because at the large-scale, self-aggregation effects dominate aggregation-hostile effects of cold pools, yield-

ing a radiatively driven deep overturning circulation that dries out the subsiding free troposphere, suppressing convection (Jeevanjee & Romps, 2013; C. Muller et al., 2022). While these general characteristics of a coupling between circulation and humidity through aggregation appear robust across a variety of studies using various cloud-resolving models (C. Muller & Bony, 2015; Wing et al., 2017), significant differences among models remain in the vertical structure of humidity, clouds, and circulation (Wing et al., 2018).

Recently, Sokol and Hartmann (2022) point out such differences in the ensemble of cloud-resolving RCE-MIP (RCE-model intercomparison project) simulations, highlighting a coupling of the congestus mode and convective aggregation. They find that about half the models participating within RCE-MIP produce a mid-level circulation that is driven by enhanced radiative cooling from moisture and cloudiness detrained around 0° C. Using a 2D cloud-resolving model they performed a small ensemble of RCE simulations within which they find a positive feedback between enhanced mid-level moisture detrainment and convective aggregation. They argue that reduced upper tropospheric moisture associated with more aggregated convection increases radiatively driven mid-level moisture divergence, enhancing mid-level subsidence and circulation strength at the expense of the deep overturning. This raises the question whether variations of the tropical large-scale overturning circulation associated with variability in mid-level moisture can also be observed in more realistic settings and whether enhanced mid-level moisture really is sourced from the convection.

Schulz and Stevens (2018) were the first to look at observations of the tropical atmosphere through the lens of "moisture space", a commonly used technique in RCE studies to enable a low-dimensional view of large-scale circulations driving moisture convergence and self-aggregation. Based on single point, but long-term measurements on Barbados, their results confirmed previous RCE studies (Bretherton et al., 2005; Jeevanjee & Romps, 2013; C. Muller & Bony, 2015) in how radiatively driven low-level circulations condition the atmosphere for deep convection. However, due to the local nature of their study, effects of enhanced mid-level moisture on the circulation and on convective aggregation may have been missed. In fact, other observational studies over the Atlantic, with less of a focus on circulation, have previously highlighted layers of increased mid-tropospheric moisture over the tropical Atlantic (Johnson et al., 1996; Stevens, 2017; Gutleben, Groß, Wirth, Emde, & Mayer, 2019; Gutleben et al., 2020; Fildier et al., 2023).

Here, our approach to test the RCE-based results of Sokol and Hartmann (2022) is to, in a first step, look for mid-tropospheric moist layers, which we refer to as elevated moist layers (EMLs), throughout the tropics. We do so based on one year of ERA5 reanalysis data, to which we apply a previously introduced EML identification method (Prange et al., 2021). We then characterise the seasonal dependence of EML occurrence over different ocean basins (Sect. 3.1) and exploit the strong dependence found over the Atlantic to examine whether the coupling between EML occurrence and the large-scale overturning circulation is similar to results from RCE (Sect 3.2). Finally, we characterise the spatio-temporal structure of EMLs around the Atlantic summer ITCZ (inter-tropical convergence zone) through a Hovmoller analysis and examine whether EMLs are actually sourced from the ITCZ (Sect. 3.3).

2 Data and methods

2.1 Reanalysis data

We use ECMWF Reanalysis v5 (ERA5) atmospheric data for the year 2021 on 0.25 ° horizontal resolution, 137 vertical levels and interpolated from hourly to 3-hourly intervals (Hersbach et al., 2020). We choose ERA5 since it previously showed a good capability in capturing EMLs when collocated with in-situ soundings, superior to two hyper-

spectral satellite retrieval products (Prange et al., 2023). We only consider data within 30° S to 30° N.

2.2 Moist layer identification

Our analysis builds upon an identification method for EMLs that enables a quantitative definition of what we consider an EML. The method is slightly modified from that proposed by Prange et al. (2021) where a vertically smooth reference profile is defined for each water vapor profile of interest by fitting a second-order polynomial against the profile of the logarithmic water vapor volume mixing ratio (VMR). Here, we adjusted the method in two ways. Firstly, the fitted profile is forced to match the VMR at the top of the mixed layer at around 950 hPa rather than at the surface to avoid a dry bias in the lower free troposphere. Secondly, the reference profile is transformed into relative humidity (RH) using the temperature and pressure profiles of the respective dataset. Positive humidity anomalies are then identified and characterised by means of strength, height and thickness in RH rather than VMR, which has the benefit that EMLs from different heights are more comparable.

We identify EMLs by applying thresholds with regard to the three EML characterization metrics. The EML strength is defined by the maximum RH anomaly within the layer. The layer is considered if EML strength exceeds 30 % of RH anomaly. The top and bottom of the anomalous layer are defined as the levels where the RH anomaly reduces to < 10 %. The anomaly thickness is defined as the pressure difference between the anomaly top and bottom. We only consider anomalies with thickness > 50 hPa and < 400 hPa as EMLs to filter small fluctuations and vertically extended anomalies that are rather a vertically constant bias than a layer. The EML height is defined as the RH anomaly's mean pressure, weighted by the anomalous RH at each level. We mainly consider mid-tropospheric EMLs with altitudes between 500 to 700 hPa.

Fig. 1 showcases an example of a mid-tropospheric EML. In Fig. 1c the positive RH anomaly against the fitted reference profile shaded in blue is characterized by a strength of 57 %, a thickness of 145 hPa, and an altitude of 590 hPa. The EML is found in a predominantly easterly flow (Fig. 1a). The mid-tropospheric EML extends meridionally between around 18° N to 5° N where a deep convective cell is found in the meridional cross-section of RH anomaly (Fig. 1b). The EML shows an increase in height with distance from the deep convection, which is also found in the 316 K isentrope highlighted by the black contour, supporting that the moisture may have detrained isentropically. However, the meridional flow component that could be driven by convective detrainment is negligible compared to the strong easterly mean flow, indicating that the moist layer has rather been advected with the easterlies. We elaborate on the emergence of EMLs over the Atlantic in Sect. 3.3.

2.3 Moisture space

A commonly used technique to distinguish the major dynamical regimes of moist convective regions and dry subsiding regions of the tropics is to sort data into bins of a vertically integrated measure of moisture (Bretherton et al., 2005; Schulz & Stevens, 2018; Lang et al., 2021; Sokol & Hartmann, 2022). The advantage is that the dimensionality is reduced from three spatiotemporal dimensions (x, y, t) to one dimension of moisture. This avoids problems with spatio-temporal shifts of circulation features and enables a simplified view at characteristics of the general circulation and humidity distribution in the tropics.

Here, we define the moisture space by sorting the data into 50 bins of IWV (integrated water vapor), with the bin-edges being defined by equi-distant percentiles of IWV to assure an even distribution of datapoints across bins. In our analysis, we consider the

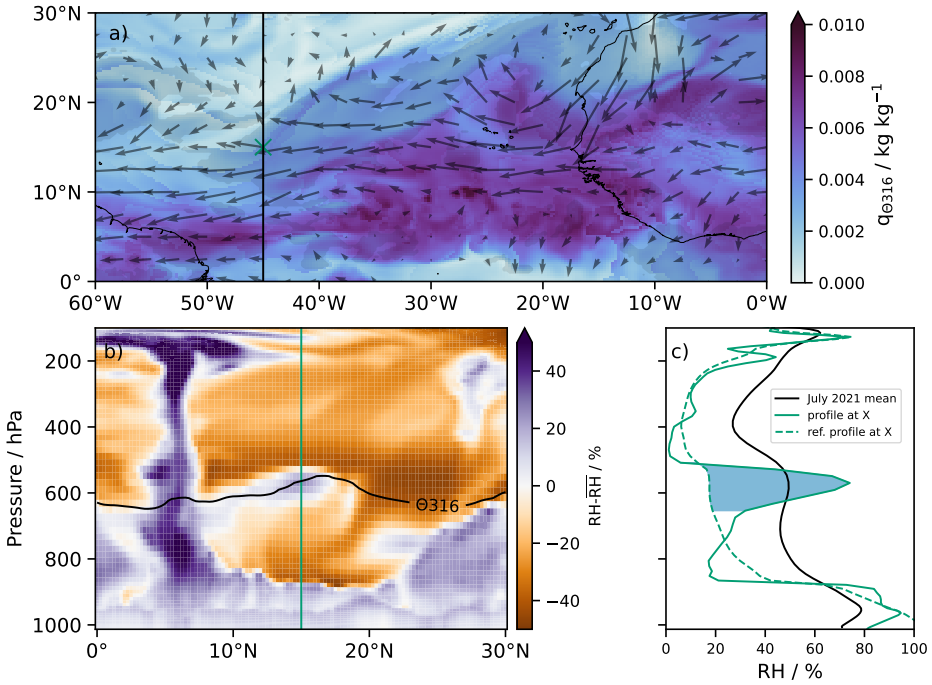

Figure 1. Overview of an EML case in ERA5 over the Northern Atlantic on July 19th, 2021 at 6 am UTC. a) shows mid-tropospheric specific humidity and flow along the 316 K isentrope. b) shows a meridional cross-section at 45° W (along black line in panel a) of RH anomaly with respect to the monthly mean. Black contour in b) highlights the 316 K isentrope. c) shows monthly mean RH profile in black, the instanteous RH profile at 15° N, 45° W, (green cross in a), green line b)) and fitted reference profile used for identifying EML. Blue shaded area denotes identified RH anomaly that is characterized by anomaly strength, thickness, and height.

moisture space integrated over the Atlantic and for single months. In this case, every bin in moisture space contains about 200,000 vertical profiles, which is plenty to obtain robust statistics to an accuracy of 0.1 % RH (Lang et al., 2021). We quantify the circulation in moisture space by means of the stream function $\Psi(p)$ as defined by Sokol and Hartmann (2022).

3 Results

3.1 Global moist layer distribution and annual cycle

By applying our method for EML identification described in Sect. 2.2 to the ERA5 data and filtering only for mid-tropospheric EMLs between 500 to 700 hPa we obtain global monthly distributions of EML occurrence rates for the year 2021 shown in Fig. 2. Overall, EML occurrence varies significantly in both zonal and meridional directions and over the Atlantic also by season. In the west and east Pacific, seasonal variability is small, but a persistent regional maximum in EML occurrence is found to the West of Peru. In this usually dry region of persistent free-tropospheric subsidence the EMLs may significantly alter the radiation budget, which can affect entraintment rates of low-level stratocumulus clouds (Stevens et al., 2003; Stevens & Brenguier, 2009). Maxima in EML occurrence are also found in regions around the precipitation bands, particularly around the Atlantic ITCZ (inter-tropical convergence zone) in July.

We find relatively low EML occurrence rates within regions of high rainfall (red shading) such as the Western Pacific where moisture is known to be detrained from deep convection near 0° C (Johnson et al., 1996). However, since RH is close to 80 % throughout the column in these regions due to the ubiquity of deep convection (Johnson et al., 1999; Romps, 2014), we do not identify this moisture as EMLs. This is desirable in our assessment of EML-circulation coupling since detrained mid-level moisture embedded in a nearly saturated atmospheric column does not have a strong effect on radiative cooling and hence circulation (Pierrehumbert, 1998; Fildier et al., 2023).

To further study the interaction of EMLs and convection, we explore the seasonal dependence of EMLs around the Atlantic ITCZ. In July, when the ITCZ shows the most intense rainfall and organized convection (Biasutti et al., 2003; Hohenegger & Jakob, 2020), EML occurrence is about double its value in January. This supports the idea of a coupling between convective organization and mid-tropospheric moisture detrainment as suggested by Sokol and Hartmann (2022). In the following, we examine whether this seasonal dependence of EML occurrence over the Atlantic goes along with a change in the overturning circulation that is consistent with RCE, or whether other moisture sources are at play.

3.2 Moist layer coupling to the large-scale circulation over the Atlantic

The annual cycle in EML occurrence over the tropical Atlantic is reflected in the monthly mean RH structure depicted in moisture space in Fig. 3a and b. While the mid-troposphere is mostly dry throughout the subsiding IWV regimes in January (i.e. IWV percentile < 95), a secondary RH maximum emerges around 600 hPa in July that extends throughout subsiding moisture regimes. This feature is similar to some models in the RCE-MIP comparison (e.g. UCLA-CRM and SAM-P3) shown by Sokol and Hartmann (2022). With the change to a more moist subsiding mid-troposphere in July we also observe a shift from a deep overturning circulation in January (Fig. 3a) to a more bottom-heavy circulation in July (Fig. 3b). The circulation in July is vertically constrained by the height of the mid-tropospheric RH maximum where radiative cooling is enhanced, consistent with the idea of a divergent moisture outflow feedback, as suggested by Sokol and Hartmann (2022). To start addressing whether this concurrent shift of humidity structure and circulation through such a feedback is causal, we now shift our perspective from

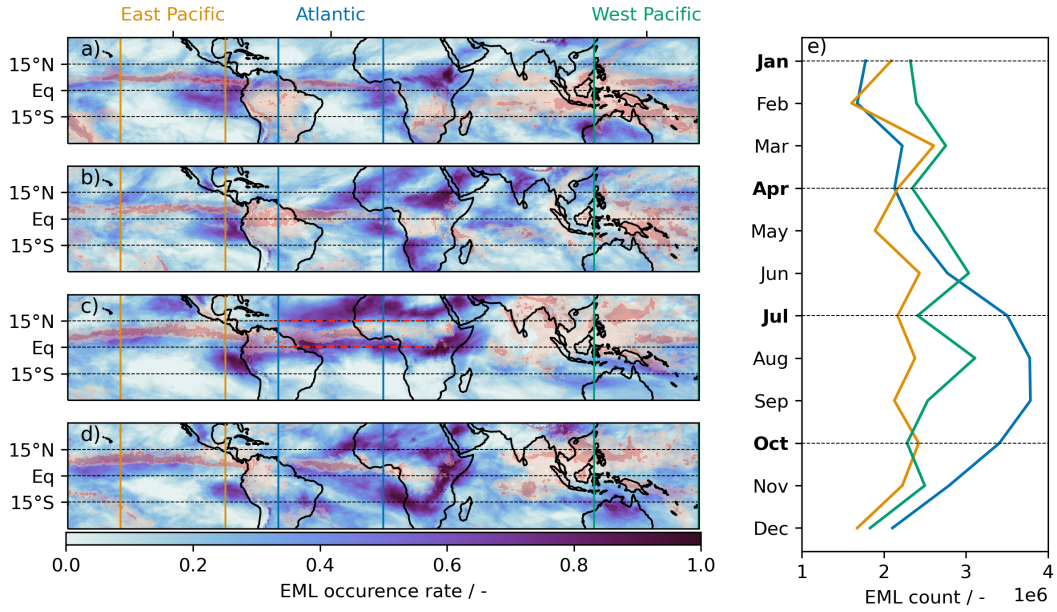

Figure 2. a) to d) show maps of monthly mid-tropospheric EML occurrence rates based on ERA5, i.e. the ratio of EMLs to the number of timesteps of the month. Maps are shown for January, April, July and October. Red contours on maps show 75th and 95th percentiles of rain rate to indicate convective activity. Red dashed lines on c) indicate cross-sections of Hovmoller diagrams in Fig. 4. EML occurrences are summed up over different ocean areas within 60°×60° longitude/latitude quadrants (land-filtered) and their annual evolution is shown panel e).

moisture space to zonal means to account for known meridional asymmetries of circulation and humidity with respect to the deep convection that is mostly occurring within the Atlantic ITCZ (Fig 3c-h).

On the zonal mean we observe the Hadley circulation (Fig. 3e+f), which in January and July is known to be dominated by a strong cross-equatorial Hadley cell with its subsiding branch on the respective winter hemisphere (e.g. Peixoto, 1992; Trenberth et al., 2000). This asymmetry in subsidence yields a more dry free troposphere on the winter hemisphere, which is also reflected in the zonal means of IWV (Fig. 3c+d). The circulations in moisture space (Fig. 3a+b) mostly reflect the respective cross-equatorial Hadley cells since they are the main source of large-scale overturning over the Atlantic (Peixoto, 1992). Hence, to explain the bottom-heaviness of the moisture space circulation in July, we have to consider the moisture field within the July cross-equatorial Hadley cell. Fig. 3h shows how in July EMLs occur abundantly North and South of the Atlantic ITCZ, however, only the Southern ones are embedded within the Hadley cell and show a direct circulation coupling through a mid-level circulation ($-24\,\mathrm{GTs}^{-1}\times10$ isoline). We conclude that the absence of EMLs north of the ITCZ in January allows for a deep circulation in moisture space while the ubiquity of EMLs south of the ITCZ in July yields a more bottom-heavy circulation.

3.3 Emergence of moist layers around the Atlantic summer ITCZ

We track mid-tropospheric EMLs around the Atlantic summer ITCZ through Hovmoller diagrams by applying our method for EML identification (Sect. 2.2) along the zonal cross-sections of the Atlantic and Africa between 60° W to 20° E at the equator (i.e. south of the ITCZ, Fig. 4a) and at 15° N (i.e. north of the ITCZ, Fig. 4b) over the month of

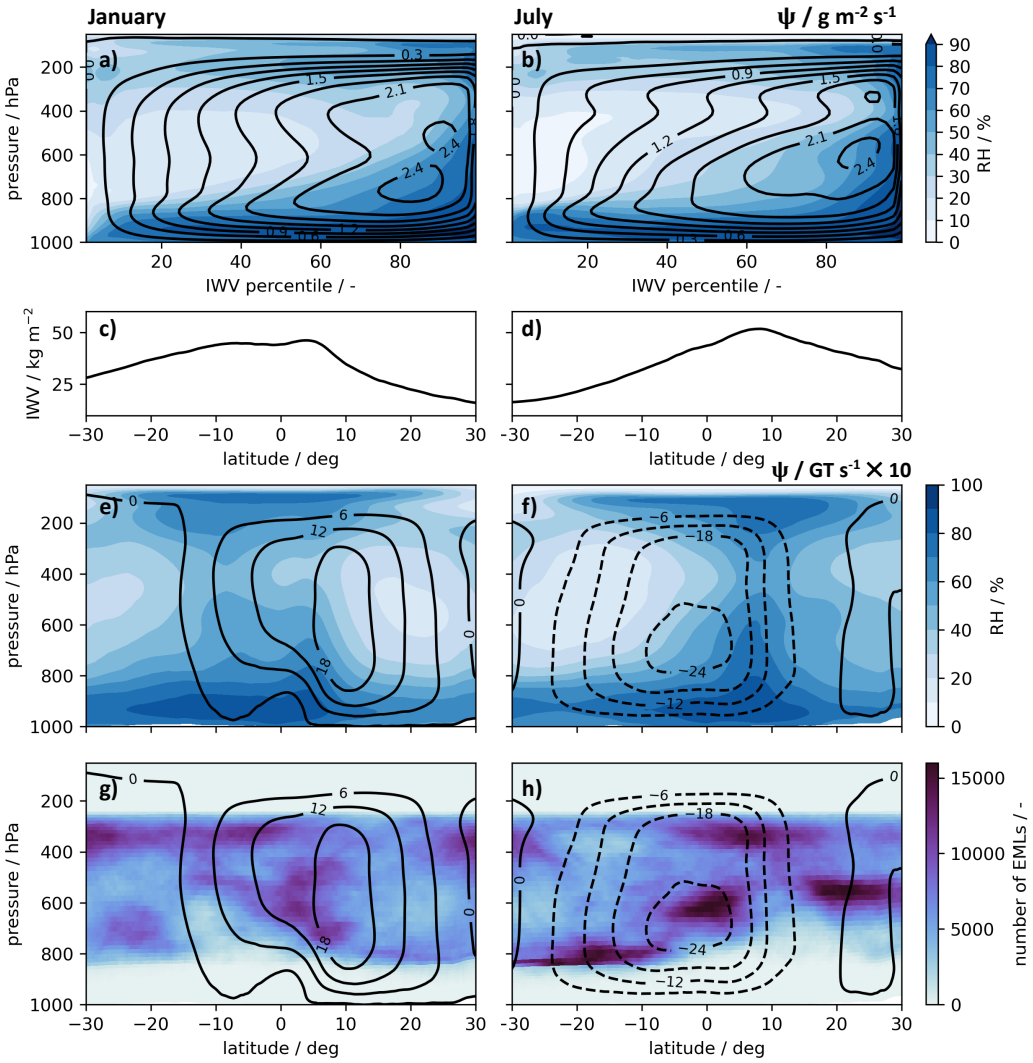

Figure 3. a) and b) show mean tropical Atlantic RH structure and circulation in terms of mass stream function Ψ in moisture space for January and July, respectively. c) to h) show zonal means over Atlantic (60° W to 0° W) of IWV, RH, stream function and number of EMLs for January (left) and July (right).

July 2021. The Hovmoller diagrams also indicate the direction of meridional wind through hatched contours, revealing whether EMLs are embedded in southerly or northerly flow. Having found that the EMLs at the equator are embedded within the cross-equatorial Hadley cell (Fig. 3h) while the northern EMLs are not, we now examine at which spatial and temporal scales EMLs emerge and live and whether the occurring EMLs coincide with a meridional flow, that is indicative of the EML being detrained from the ITCZ.

The EMLs at the equator (Fig. 4) emerge and decay throughout the zonal cross-section. EMLs are present in the east over the Gulf of Guinea and although they have a slight easterly wind component they do not show a clear zonal propagation pattern across the Atlantic. Instead, EMLs west of the Golf of Guinea emerge over the open Atlantic and generally within a northerly meridional wind. Particularly pronounced EMLs occur around July 22nd at 30° W and around July 27th at 40° W, lasting for around 3 to 4 days and showing a slight westward propagation. Overall, we find that 73 % of EMLs on the equatorial cross-section in July are embedded in a north-easterly flow, with a mean u-wind of -4.9 $\mathrm{m\,s^{-1}}$ and v-wind of -1.3 $\mathrm{m\,s^{-1}}$, indicating that the moisture is indeed sourced from the ITCZ.

The pattern of EMLs and meridional winds on the 15° N Hovmoller diagram (Fig. 4b) differs signifcantly from the equatorial one. EMLs mostly emerge around the West African coastline near 15° W and are embedded in a stronger easterly flow with an average u-wind of -11.6 $\mathrm{m\,s^{-1}}$ within the EMLs and a more varying meridional wind that averages to -0.8 $\mathrm{m\,s^{-1}}$. This underpins our conclusion from the zonal mean analysis (Fig. 3h) where EMLs north of the ITCZ appear uncoupled to the Hadley circulation and instead suggests that the dynamics over the West African continent are key for the emergence of EMLs in the north with a strong easterly flow advecting them across the Atlantic.

In Fig. 4c we depict the July zonal mean cross-section from 20° W to the prime meridian averaging over the West African continent and the Gulf of Guinea, highlighting some main characteristics of the West African monsoon system (for a comprehensive review consider Fink et al., 2017). Around 10° N lies the West African ITCZ denoted by high RH throughout the troposphere, which is fed by a low-level south-westerly inflow of moist Atlantic air in the monsoon layer (ML) coming in from the Gulf of Guinea (Marsham et al., 2013). In addition, moisture is transported towards the ITCZ and the Sahel with the Atlantic trade winds that deflect eastward around Senegal due to the West African heat low (Lavaysse et al., 2009; Diekmann et al., 2021). This low-level moisture convergence yields intense deep convection over West Africa at around 10° N, moistening the entire column. This moistening coupled with a strongly sheared zonal mean flow from westerlies in the ML to the African Easterly Jet (AEJ) in the mid-troposphere appears as a prime producer of EMLs over the northern Atlantic in summer.

In addition, RH north of the West African ITCZ is enhanced near 500 hPa at the top of the Saharan Air Layer (SAL). This is achieved through intense daytime adiabatic mixing of low-level moist air that surges into the Saharan heat low from the south at night and dry SAL air from aloft (Parker et al., 2005; Karam et al., 2008; Marsham et al., 2013). Hence, particularly during daytime, enhanced RH and stratocumulus clouds are frequently observed at the top of the SAL (Stein et al., 2011). Fig. 2c shows a preponderance of EMLs over the Sahara, which could be explained through this mechanism. Again, the alignment of the enhanced mid-tropospheric moisture at the SAL top with the strongly sheared zonal flow associated with the AEJ contributes to the production of EMLs over the northern Atlantic in summer. A clear indication of EMLs originating from SAL airmasses is that they were coherently found with increased mineral dust concentrations (Stevens, 2017; Gutleben, Groß, & Wirth, 2019)

Finally, we want to point out how the EMLs at 15° N are transported together with patterns of alternating northerly and southerly meridional winds (Fig. 4b), which are indicative of African Easterly Waves (AEWs) that form between May and October as dis-

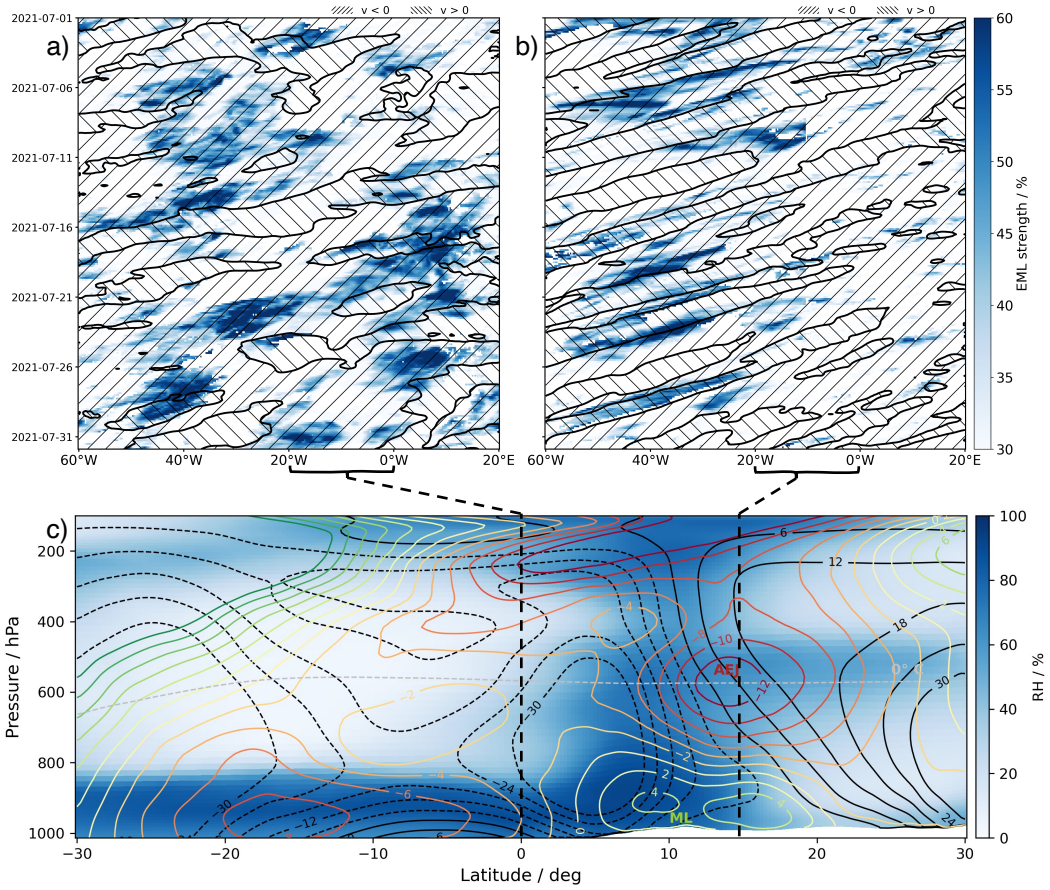

Figure 4. a) and b) show Hovmoller diagrams of EML strength and direction of meridional wind (hatched) averaged between 500 to 700 hPa along equator (a) and 15° N (b) between 60° W to 20° E (red dashed lines in Fig. 2c) for July 2021. Blue contours indicate the presence and strength of a mid-tropospheric EML. c) shows July zonal mean cross-section over West Africa and Gulf of Guinea (20° W to 0° W) of RH, stream function (black contours), zonal wind (red/green contours) and the 0° C isotherm (gray dashed contour). The positions of the Afican easterly jet (AEJ) and the monsoon layer (ML) are indicated.

turbances of the AEJ and act as predecessors of tropical cyclones (e.g. Thorncroft & Hodges, 2001; Kiladis et al., 2006; Mekonnen & Rossow, 2011). Enyew and Mekonnen (2021) highlight how RH anomalies ahead of the AEW trough may favor the AEW's development into a tropical cyclone, indicating that EMLs may play a role in predicting AEW development.

4 Conclusion

We set out to look for layers of enhanced mid-tropospheric moisture (EMLs) throughout the tropics based on one year of ERA5 data, motivated by a recently suggested coupling of aggregated convection and a radiatively driven mid-level circulation in RCE (Sokol & Hartmann, 2022). We find EML occurrence over the tropical Atlantic to have a pronounced seasonal cycle, with a minimum in winter and a maximum in summer, allow-

ing us to test the RCE-based hypotheses about a moisture-circulation coupling in realistic conditions.

The enhanced mid-level moisture over the Atlantic in July goes along with a shift to a more bottom-heavy circulation in moisture space when compared to the EML-sparse month January. However, we point out how meridional asymmetries in moisture and circulation around the convective regions can yield misleading deductions from moisture space alone. In particular, while EMLs occur north and south of the Atlantic summer ITCZ, only the southern ones are embedded within the cross-equatorial Hadley cell, coupling to the large-scale circulation. Since we find these EMLs to emerge throughout the Atlantic in a mostly northerly meridional flow from the ITCZ, we conclude that they are most likely sourced from deep convection within the ITCZ and indeed part of a radiatively driven mid-level circulation as suggested by Sokol and Hartmann (2022).

While this moisture-circulation coupling resembles RCE-based results, here we only make a qualitative argument about how this can be explained by the degree of convective aggregation and its ability to dry out the upper troposphere by referencing Hohenegger and Jakob (2020), who diagnose a more organised Atlantic ITCZ in boreal summer. Global storm resolving simulations may denote an interesting tool to more quantitatively address this since deep convective processes are resolved (Stevens et al., 2019).

North of the Atlantic summer ITCZ, EMLs are also ubiquitous but typically emerge over the West-African continent. The on average northerly meridional wind in these EMLs indicates no significant contribution of moisture detrained from the Atlantic ITCZ to the south. Instead, deep convection within the West-African ITCZ and vertical mixing of moist monsoonal air within the SAL moisten the West-African mid-troposphere, from where a sheared mean flow associated with the AEJ advects the moisture as EMLs across the Atlantic, along with AEWs. This result motivates further exploration of the coupling of EMLs and AEW development into tropical cyclones. In addition, the contributions of convective moisture sources compared to SAL mixing in producing EMLs over West Africa require further quantification. This may be addressed through further characterisation of EML dust loads as done for single cases by Gutleben, Groß, and Wirth (2019), e.g. from satellite observations or measurement campaigns. Another way to distinguish EML moisture sources is to calculate lagrangian backward trajectories, as done by Diekmann et al. (2021); Villiger et al. (2022), but specifically for a larger set of EML air parcels.

The results presented here may also have implications for constraining the clear-sky energy balance of CMIP (Climate Model Intercomparison Project) models. Recently, Feng et al. (2023) point out how biases in sub-tropical mid-tropospheric RH among CMIP6 models yield a model spread of $10\,\mathrm{W\,m^{-2}}$ in clear-sky outgoing longwave radiation (OLR). This may be surprising at first given that most uncertainty in such models is typically associated with clouds (Stevens & Bony, 2013; Bony et al., 2015). However, it becomes perceivable when considering how large the spread of mid-tropospheric RH and circulation is in cloud-resolving RCE models as discussed by Sokol and Hartmann (2022). In addition, the added complexity of moisture sources and circulation coupling in more realistic settings discussed here might be difficult to capture by coarse models. Assessing EML characteristics of CMIP6 models with reference to the results presented here may help in narrowing down sources of mid-tropospheric RH biases between models and reduce OLR biases.

Open Research Section

EML characteristics derived from ERA5 data is published on Zenodo, together with the analysis code (Prange et al., 2024).

Acknowledgments

This research was funded by the Deutsche Forschungsgemeinschaft (DFG, German Research Foundation) under Germany's Excellence Strategy—EXC 2037 "CLICCS—Climate, Climatic Change, and Society"—Project Number: 390683824, contribution to the Center for Earth System Research and Sustainability (CEN) of Universität Hamburg.

I thank Sandrine Bony for her initiating thoughts about a coupling to tropical waves and Nedjeljka Žagar for offering further insight on analysis methods of AEWs. I thank Lukas Kluft for technical assistance in wrangling with the data.

References

Bellon, G., Treut, H. L., & Ghil, M. (2003). Large-scale and evaporation-wind feedbacks in a box model of the tropical climate. *Geophysical Research Letters*, *30*(22). doi: 10.1029/2003gl017895

Biasutti, M., Battisti, D. S., & Sarachik, E. S. (2003, August). The Annual Cycle over the Tropical Atlantic, South America, and Africa. *Journal of Climate*, *16*(15), 2491–2508. doi: 10.1175/1520-0442(2003)016⟨2491:TACOTT⟩2.0.CO;2

Bony, S., Stevens, B., Frierson, D. M. W., Jakob, C., Kageyama, M., Pincus, R., ... Webb, M. J. (2015). Clouds, circulation and climate sensitivity. *Nature Geoscience*, *8*(4), 261–268. doi: 10.1038/ngeo2398

Bretherton, C. S., Blossey, P. N., & Khairoutdinov, M. (2005). An Energy-Balance Analysis of Deep Convective Self-Aggregation above Uniform SST. *Journal of the Atmospheric Sciences*, *62*(12), 4273–4292. doi: 10.1175/jas3614.1

Diekmann, C. J., Schneider, M., Knippertz, P., de Vries, A. J., Pfahl, S., Aemisegger, F., ... Braesicke, P. (2021). A Lagrangian Perspective on Stable Water Isotopes During the West African Monsoon. *Journal of Geophysical Research: Atmospheres*, *126*(19), e2021JD034895. doi: 10.1029/2021JD034895

Enyew, B. D., & Mekonnen, A. (2021). The Interaction between African Easterly Waves and Different Types of Deep Convection and Its Influence on Atlantic Tropical Cyclones. *Atmosphere*, *13*(1), 5. doi: 10.3390/atmos13010005

Feng, J., Paynter, D., Wang, C., & Menzel, R. (2023, September). How atmospheric humidity drives the outgoing longwave radiation–surface temperature relationship and inter-model spread. *Environmental Research Letters*, *18*(10), 104033. doi: 10.1088/1748-9326/acfb98

Fildier, B., Muller, C., Pincus, R., & Fueglistaler, S. (2023). How Moisture Shapes Low-Level Radiative Cooling in Subsidence Regimes. *AGU Advances*, *4*(3). doi: 10.1029/2023av000880

Fink, A. H., Engel, T., Ermert, V., van der Linden, R., Schneidewind, M., Redl, R., ... Janicot, S. (2017). Mean Climate and Seasonal Cycle. In *Meteorology of Tropical West Africa* (pp. 1–39). John Wiley & Sons, Ltd. doi: 10.1002/9781118391297.ch1

Gutleben, M., Groß, S., & Wirth, M. (2019). Cloud macro-physical properties in Saharan-dust-laden and dust-free North Atlantic trade wind regimes: A lidar case study. *Atmospheric Chemistry and Physics*, *19*(16), 10659–10673. doi: 10.5194/acp-19-10659-2019

Gutleben, M., Groß, S., Wirth, M., Emde, C., & Mayer, B. (2019). Impacts of Water Vapor on Saharan Air Layer Radiative Heating. *Geophysical Research Letters*, *46*(24), 14854–14862. doi: 10.1029/2019gl085344

Gutleben, M., Groß, S., Wirth, M., & Mayer, B. (2020). Radiative effects of long-range-transported Saharan air layers as determined from airborne lidar measurements. *Atmospheric Chemistry and Physics*, *20*(20), 12313–12327. doi: 10.5194/acp-20-12313-2020

Hersbach, H., Bell, B., Berrisford, P., Hirahara, S., Horányi, A., Muñoz-Sabater, J.,

... Thépaut, J.-N. (2020). The ERA5 global reanalysis. *Quarterly Journal of the Royal Meteorological Society*, *146*(730), 1999–2049. doi: 10.1002/qj.3803

Hohenegger, C., & Jakob, C. (2020). A Relationship Between ITCZ Organization and Subtropical Humidity. *Geophysical Research Letters*, *47*(16), e2020GL088515. doi: 10.1029/2020GL088515

Jeevanjee, N., & Romps, D. M. (2013). Convective self-aggregation, cold pools, and domain size. *Geophysical Research Letters*, *40*(5), 994–998. doi: 10.1002/grl.50204

Johnson, R. H., Ciesielski, P. E., & Hart, K. A. (1996, July). Tropical Inversions near the 0°C Level. *Journal of the Atmospheric Sciences*, *53*(13), 1838–1855. doi: 10.1175/1520-0469(1996)053⟨1838:TINTL⟩2.0.CO;2

Johnson, R. H., Rickenbach, T. M., Rutledge, S. A., Ciesielski, P. E., & Schubert, W. H. (1999). Trimodal Characteristics of Tropical Convection. *Journal of Climate*, *12*(8), 2397–2418. doi: 10.1175/1520-0442(1999)012⟨2397:tcotc⟩2.0.co;2

Karam, D. B., Flamant, C., Knippertz, P., Reitebuch, O., Pelon, J., Chong, M., & Dabas, A. (2008). Dust emissions over the Sahel associated with the West African monsoon intertropical discontinuity region: A representative case-study. *Quarterly Journal of the Royal Meteorological Society*, *134*(632), 621–634. doi: 10.1002/qj.244

Kelly, M. A., & Randall, D. A. (2001). A Two-Box Model of a Zonal Atmospheric Circulation in the Tropics. *Journal of Climate*, *14*(19), 3944–3964. doi: 10.1175/1520-0442(2001)014⟨3944:atbmoa⟩2.0.co;2

Kiladis, G. N., Thorncroft, C. D., & Hall, N. M. J. (2006, September). Three-Dimensional Structure and Dynamics of African Easterly Waves. Part I: Observations. *Journal of the Atmospheric Sciences*, *63*(9), 2212–2230. doi: 10.1175/JAS3741.1

Lang, T., Naumann, A. K., Stevens, B., & Buehler, S. A. (2021). Tropical Free-Tropospheric Humidity Differences and Their Effect on the Clear-Sky Radiation Budget in Global Storm-Resolving Models. *Journal of Advances in Modeling Earth Systems*, *13*(11). doi: 10.1029/2021ms002514

Larson, K., Hartmann, D. L., & Klein, S. A. (1999). The Role of Clouds, Water Vapor, Circulation, and Boundary Layer Structure in the Sensitivity of the Tropical Climate. *Journal of Climate*, *12*(8), 2359–2374. doi: 10.1175/1520-0442(1999)012

Lavaysse, C., Flamant, C., Janicot, S., Parker, D. J., Lafore, J.-P., Sultan, B., & Pelon, J. (2009, August). Seasonal evolution of the West African heat low: A climatological perspective. *Climate Dynamics*, *33*(2), 313–330. doi: 10.1007/s00382-009-0553-4

Marsham, J. H., Dixon, N. S., Garcia-Carreras, L., Lister, G. M. S., Parker, D. J., Knippertz, P., & Birch, C. E. (2013). The role of moist convection in the West African monsoon system: Insights from continental-scale convection-permitting simulations. *Geophysical Research Letters*, *40*(9), 1843–1849. doi: 10.1002/grl.50347

Mekonnen, A., & Rossow, W. B. (2011). The Interaction Between Deep Convection and Easterly Waves over Tropical North Africa: A Weather State Perspective. *Journal of Climate*, *24*(16), 4276–4294. doi: 10.1175/2011jcli3900.1

Miller, R. L. (1997). Tropical Thermostats and Low Cloud Cover. *Journal of Climate*, *10*(3), 409–440. doi: 10.1175/1520-0442(1997)010⟨0409:ttalcc⟩2.0.co;2

Muller, C., & Bony, S. (2015). What favors convective aggregation and why? *Geophysical Research Letters*, *42*(13), 5626–5634. doi: 10.1002/2015gl064260

Muller, C., Yang, D., Craig, G., Cronin, T., Fildier, B., Haerter, J. O., ... Sherwood, S. C. (2022). Spontaneous Aggregation of Convective Storms. *Annual Review of Fluid Mechanics*, *54*(1), 133–157. doi: 10.1146/annurev-fluid-022421-011319

Muller, C. J., & Held, I. M. (2012). Detailed Investigation of the Self-Aggregation

of Convection in Cloud-Resolving Simulations. *Journal of the Atmospheric Sciences*, *69*(8), 2551–2565. doi: 10.1175/jas-d-11-0257.1

Parker, D. J., Thorncroft, C. D., Burton, R. R., & Diongue-Niang, A. (2005). Analysis of the African easterly jet, using aircraft observations from the JET2000 experiment. *Quarterly Journal of the Royal Meteorological Society*, *131*(608), 1461–1482. doi: 10.1256/qj.03.189

Peixoto, A. H. O., Jose P. (1992). *Physics of Climate* (1st ed.). American Institute of Physics Melville, NY.

Pierrehumbert, R. T. (1995). Thermostats, Radiator Fins, and the Local Runaway Greenhouse. *Journal of the Atmospheric Sciences*, *52*(10), 1784–1806. doi: 10.1175/1520-0469(1995)052

Pierrehumbert, R. T. (1998). Lateral mixing as a source of subtropical water vapor. *Geophysical Research Letters*, *25*(2), 151–154. doi: 10.1029/97GL03563

Prange, M., Brath, M., & Buehler, S. A. (2021). Are elevated moist layers a blind spot for hyperspectral infrared sounders? A model study. *Atmospheric Measurement Techniques*, *14*(11), 7025–7044. doi: 10.5194/amt-14-7025-2021

Prange, M., Buehler, S. A., & Brath, M. (2023). How adequately are elevated moist layers represented in reanalysis and satellite observations? *Atmospheric Chemistry and Physics*, *23*(1), 725–741. doi: 10.5194/acp-23-725-2023

Prange, M., Stevens, B., & Buehler, S. A. (2024). *Supplementary data for "Emergence and circulation coupling of moist layers over the tropical Atlantic".* Zenodo [Dataset, Software]. doi: 10.5281/zenodo.10667051

Romps, D. M. (2014). An Analytical Model for Tropical Relative Humidity. *Journal of Climate*, *27*(19), 7432–7449. doi: 10.1175/jcli-d-14-00255.1

Schulz, H., & Stevens, B. (2018). Observing the Tropical Atmosphere in Moisture Space. *Journal of the Atmospheric Sciences*, *75*(10), 3313–3330. doi: 10.1175/jas-d-17-0375.1

Sokol, A. B., & Hartmann, D. L. (2022). Congestus Mode Invigoration by Convective Aggregation in Simulations of Radiative-Convective Equilibrium. *Journal of Advances in Modeling Earth Systems*, *14*(7), e2022MS003045. doi: 10.1029/2022MS003045

Stein, T. H. M., Parker, D. J., Delanoë, J., Dixon, N. S., Hogan, R. J., Knippertz, P., ... Marsham, J. H. (2011). The vertical cloud structure of the West African monsoon: A 4 year climatology using CloudSat and CALIPSO. *Journal of Geophysical Research: Atmospheres*, *116*(D22). doi: 10.1029/2011JD016029

Stevens, B. (2017, June). Clouds unfazed by haze. *Nature*, *546*(7659), 483–484. doi: 10.1038/546483a

Stevens, B., & Bony, S. (2013). What Are Climate Models Missing? *Science*, *340*(6136), 1053–1054. doi: 10.1126/science.1237554

Stevens, B., & Brenguier, J.-L. (2009, February). Cloud-controlling Factors: Low Clouds. In J. Heintzenberg & R. J. Charlson (Eds.), *Clouds in the Perturbed Climate System: Their Relationship to Energy Balance, Atmospheric Dynamics, and Precipitation* (p. 0). The MIT Press. doi: 10.7551/mitpress/9780262012874.003.0008

Stevens, B., Lenschow, D. H., Faloona, I., Moeng, C.-H., Lilly, D. K., Blomquist, B., ... Thornton, D. (2003). On entrainment rates in nocturnal marine stratocumulus. *Quarterly Journal of the Royal Meteorological Society*, *129*(595), 3469–3493. doi: 10.1256/qj.02.202

Stevens, B., Satoh, M., Auger, L., Biercamp, J., Bretherton, C. S., Chen, X., ... Zhou, L. (2019). DYAMOND: The DYnamics of the Atmospheric general circulation Modeled On Non-hydrostatic Domains. *Progress in Earth and Planetary Science*, *6*(1), 61. doi: 10.1186/s40645-019-0304-z

Thorncroft, C., & Hodges, K. (2001, March). African Easterly Wave Variability and Its Relationship to Atlantic Tropical Cyclone Activity. *Journal of Climate*,

14(6), 1166–1179. doi: 10.1175/1520-0442(2001)014⟨1166:AEWVAI⟩2.0.CO;2

Trenberth, K. E., Stepaniak, D. P., & Caron, J. M. (2000, November). The Global Monsoon as Seen through the Divergent Atmospheric Circulation. *Journal of Climate*, *13*(22), 3969–3993. doi: 10.1175/1520-0442(2000)013⟨3969:TGMAST⟩2.0.CO;2

Villiger, L., Wernli, H., Boettcher, M., Hagen, M., & Aemisegger, F. (2022). Lagrangian formation pathways of moist anomalies in the trade-wind region during the dry season: Two case studies from EUREC4A. *Weather and Climate Dynamics*, *3*(1), 59–88. doi: 10.5194/wcd-3-59-2022

Wing, A. A., Emanuel, K., Holloway, C. E., & Muller, C. (2017). Convective Self-Aggregation in Numerical Simulations: A Review. *Surveys in Geophysics*, *38*(6), 1173–1197. doi: 10.1007/s10712-017-9408-4

Wing, A. A., Reed, K. A., Satoh, M., Stevens, B., Bony, S., & Ohno, T. (2018). Radiative–convective equilibrium model intercomparison project. *Geoscientific Model Development*, *11*(2), 793–813. doi: 10.5194/gmd-11-793-2018